Available online at www.sciencedirect.com
ScienceDirect
Ceramics International 35 (2009) 3229–3234
CERAMICS INTERNATIONAL
www.elsevier.com/locate/ceramint

Composition and properties of glass obtained from Early Cretaceous Sidi Aich sands (central Tunisia)

W. Hajjaji [a,b], K. Jeridi [a], P. Seabra [b], F. Rocha [c], J.A. Labrincha [b,*], F. Jamoussi [a]

[a] *Géoressources Laboratory, CERTE BP 273, 8020 Soliman, Tunisia*
[b] *Ceramics and Glass Engineering Dept & CICECO, University of Aveiro, 3810-193 Aveiro, Portugal*
[c] *Geobiotec, Geosciences Dept, University of Aveiro, 3810-193 Aveiro, Portugal*

Received 6 February 2009; received in revised form 5 March 2009; accepted 18 May 2009
Available online 18 June 2009

Abstract

The present work describes the chemical–mineralogical characterization of Barremian sand deposits. These Sidi Aich sands are observed exclusively in central Tunisia; in the Central Atlas two major domains might be discriminated: north–south axis and southern Atlas. In the collected raw samples, quartz and potassic feldspars are depicted with percentages that reach 30 wt.%. The chemical and XRD analyses confirm the existence of K-feldspars. These compounds are known fluxing agents. Since the amount in heavy minerals (<0.36 wt.%) and Fe_2O_3 (<0.71 wt.%) is relatively low, their interest for glass manufacturing is high.

In accordance, semi-industrial tests were carried out to produce glass. The obtained bodies were investigated by XRD, attempting to detect the crystalline phases that can appear and influence the technological behaviour of these glasses. Mechanical properties distinguished SMS and SAT glasses when the others are conditioned by microfractures that could be related to annealing stage. The investigation also concerned the colours exhibited by final products (green to amber). This aspect is dependent on the amount of iron and its redox states; ferrous (Fe^{2+})/ferric iron (Fe^{3+}) which is here detected in UV–vis–NIR spectra of different tested glasses.

Keywords: C. Mechanical properties; C. Colour; D. Glass; Barremian sands

1. Introduction

According to ASTM Standards glass is an inorganic product of fusion which has been cooled to a rigid condition without crystallization. Nevertheless, even though it was used since about 4 millenniums, it remains a material difficult to define perfectly. Nowadays, it is one of the most used materials in a multiplicity of fields [1,2]. Soda-lime-silicate glasses are the most common and widely used, since they are cheap, easily melted and shaped. In its production the used raw materials are sodium carbonate, calcite or dolomite, and silica sand as the major constituent [2].

In Tunisia the real interest derived to sand is its association as good hydrocarbon reservoir. So the only studies undertaken were essentially focused in sedimentology, tectonic and paleogeography like those reported by Burollet [3,4], M'Rabet [5], and Ben Ferjani et al. [6]. Normally in Tunisia, the valorisation of sand in other domains is not widely reported. Some works conducted by Jamoussi [7] tackled the subject of using the sand of Gafsa and other regions in the glass industry. These trials seem not to be well succeeded since Tunisian glass producers continue to import the sand from other countries.

This paper reports the results of an experimental study performed on Early Cretaceous Sidi Aich sands. These detrital deposits are found in the central part of Tunisia, in two major domains, and they cover large areas. Central Atlas is characterized by a series of NE–SW folds separated by synclinals filled by Neogene and Quaternary sediments when meridional Atlas is formed by E–W folds [8,9]. These structures localized in the north of the Saharian platform are affected by a system of NW–SE and E–W faults forming a series of pull-a-part basins accommodating detrital sediments [10]. In this context, the regressive eustatic period occurred in Barremian favoured the sedimentation of Sidi Aich sands up to Bouhedma clays. These sands defined by Burollet [3] were sampled in the localities of Jebel Meloussi (SMS), Jebel Attaf

* Corresponding author. Tel.: +351 234370250; fax: +351 234370204.
E-mail address: jal@ua.pt (J.A. Labrincha).

0272-8842/$36.00
doi:10.1016/j.ceramint.2009.05.027

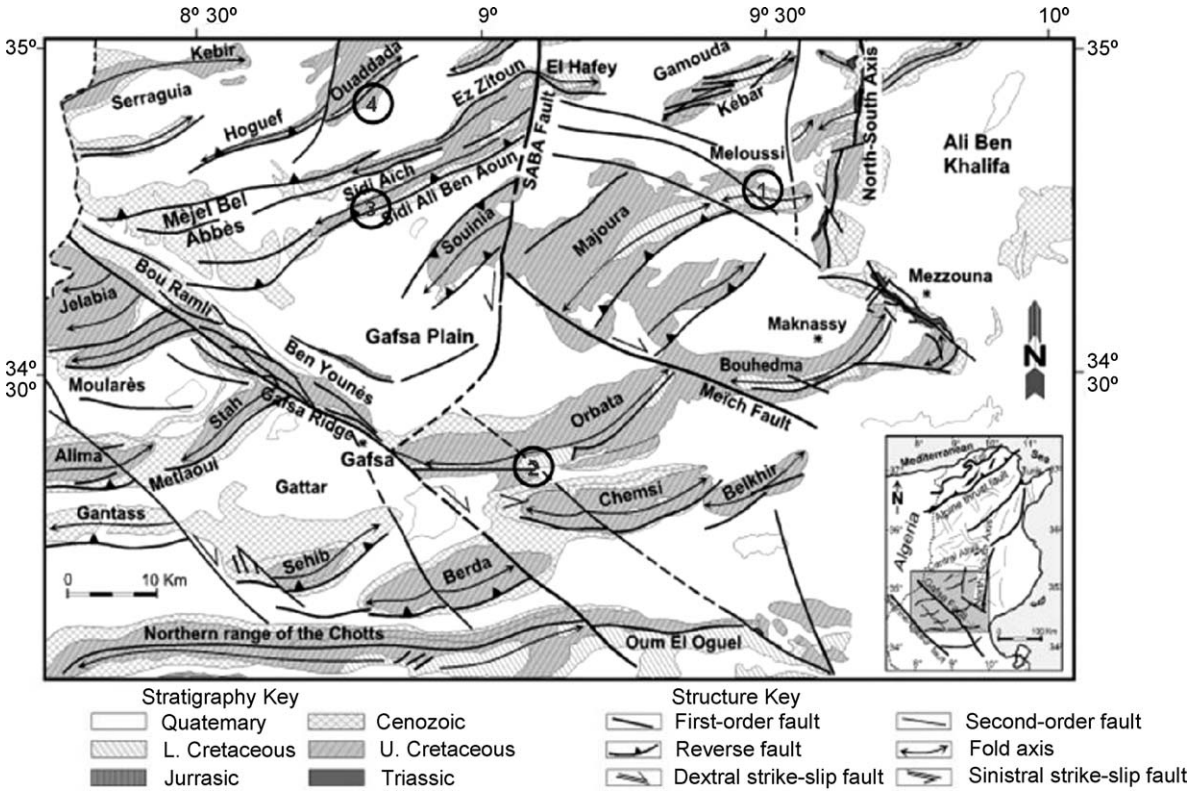

Fig. 1. Samples localisation: (1) Jebel Meloussi (SMS), (2) Jebel Attaf (SAT), (3) Jebel Sidi Aich (SBSA) and (4) Jebel Ouaddada (SBJO) (Map from Zouaghi et al. [9]).

(SAT), Jebel Sidi Aich (SBSA), and Jebel Ouaddada (SBJO) (Fig. 1). The sequence presents white fine silica sands with rare clays and carbonates intercalations. The thickness varies from a zone to another due to the diachronism affecting the inferior Late Cretaceous series [5,6].

2. Experimental

Mineralogical and major–minor chemical compositions were determined for whole-rock samples and on pre-sieved fractions. The mineralogy was determined in raw and glass materials using an X-ray Panalytical X'Pert PRO diffractometer (CuKα, $\lambda = 0.154056$ nm, 2θ range 3–60°). The collected data were processed by Panalytical X'Pert Highscore software. The existing phases were identified by X-ray powder diffraction and their relative amount was estimated by measuring the peak areas of principal reflexion [11–13]. The same method was used in the identification of heavy metals. Beforehand, components with specific gravity greater than quartz (2.65 g/cm^3) or feldspars (2.76 g/cm^3), were separated in the laboratory, by using sodium polytungstate (SPT) (specific gravity 2.82 g/cm^3) as heavy liquid. The chemical composition of these Barremian sands was estimated, on powdered samples, by X-ray fluorescence using Panalytical Axios Dispersive X-ray Fluorescence Spectrometer. The results are expressed as percent concentrations of element oxides.

The grain-size distribution was obtained via dry sieving in an AFNOR series adopted by the French normalisation system. For the fraction inferior to 63 μm, the grain-size distribution was determined by a Micromeritics 5000ET sedigraph.

The glasses were produced on laboratory tests, attempting to follow as close as possible the manufacturing scale. Batches were prepared following the fixed composition (wt.%): 71.91% SiO_2, 1.61% Al_2O_3, 12.52% Na_2O, 1.84% K_2O, 2.37% MgO and 9.75% CaO. This is a typical formulation used to produce sodium–calcium glass [14]. The different selected Barremian sands were mixed with sodium carbonate (Na_2CO_3) acting as fluxing agent, while dolomite was added to stabilize the glass against rapid chemical attack by fluids.

The mixture was wet ball-milled and then dried at 100 °C during 24 h. Then, it was fired for 4-h soaking at the maximum temperature (1600 °C). The melted liquid was poured to a metallic mould and kept for 2 h at 580 °C (annealed), aiming to relax stresses and prevent cracks formation [15].

The obtained glasses were characterized by XRD, to detect the existence of unwanted crystalline particles, and by scanning electronic microscopy (SEM - Hitachi, SU 70) to observe the microstructural details. Mechanical three-point bending tests (Shimadzu Autograph AG-IS) were carried out with a loading rate of 0.5 mm/min and finally the glasses colour was also evaluated by UV–vis–IR spectroscopy (Shimadzu UV-3100).

3. Results

3.1. Raw materials characterization

Representative samples of the four Barremian sands (SMS, SAT, SBSA, and SBJO) revealed to have a similar mineralogical composition, quartz being the dominant phase (Fig. 2). Phase's semi-quantification by XRD is given in Table 1,

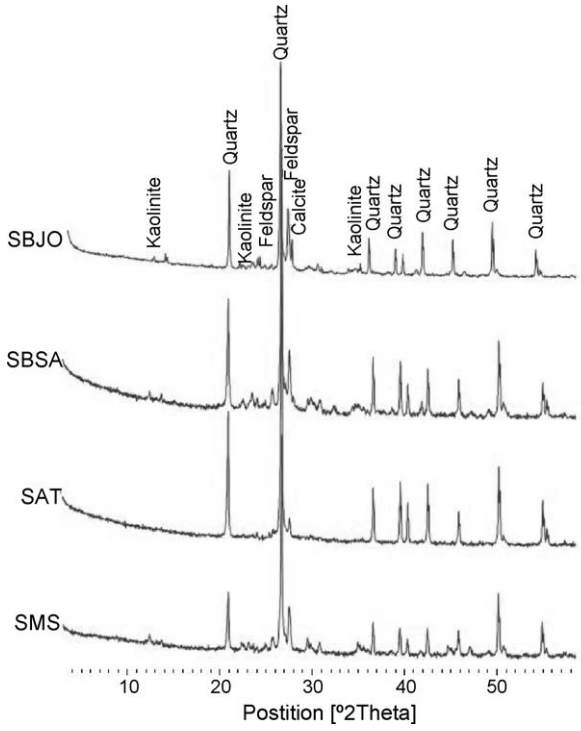

Fig. 2. XRD patterns of the studied sands.

denoting that potassic feldspar is the secondary phase, particularly relevant in SBSA and SBJO samples. Calcite and kaolinitic-type phyllosilicates are the minor detected phases. Also small quantities of heavy minerals (between 0.04 wt.% in SAT and 0.36 wt.% in SBSA) were extracted from the sand samples. Under very humid conditions, not observed in the Barremian deposits, these feldspars and ferromagnesian phases might be leached. The most significant phases detected in the 100–160 μm fraction were micas, ilmenite, tourmaline, rutile and anatase. Moreover, corundum, garnet, zircon and

Table 1
Mineralogical and chemical composition of the studied sands.

	SMS	SAT	SBSA	SBJO
Quartz	91	97.8	90.1	71.8
Feldspar	7	1.8	8.6	27.1
Calcite	1	0.4	0.9	0.5
Phyllosilicates	1	0	0.4	0.6
SiO_2	84.3	97.4	86.2	87.8
Al_2O_3	7.45	1.11	6.78	5.98
Fe_2O_3	0.71	0.37	0.54	0.35
MgO	0.08	0.06	0.10	0.42
CaO	0.26	0.01	0.02	0.25
Na_2O	0.00	0.00	0.00	0.17
K_2O	5.76	0.52	5.42	4.64
CuO	0.00	0.01	0.00	0.00
ZnO	0.00	0.00	0.01	0.00
Cr_2O_3	0.05	0.01	0.06	0.06
ZrO_2	0.14	0.07	0.05	0.03
TiO_2	0.72	0.63	0.61	0.29
P_2O_5	0.04	0.00	0.00	0.02
LOI	0.80	0.30	0.90	0.60
Total	100.32	100.49	100.69	100.61

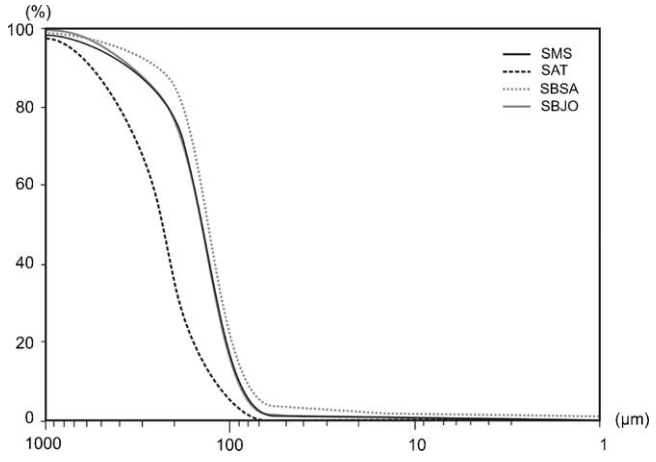

Fig. 3. Granulometric distribution of Barremian sands.

diopside were detected by XRD diffraction. Due to their small granulometry, these phases (e.g. Fe-rich) could be leached and influence the final colour of the glass [16,17].

Table 1 also gives the average chemical composition of the tested sands. It is somewhat similar in all cases, excepting SAT. In this case, the relative amount of SiO_2 is higher (97.4 wt.%), while the amount of Al_2O_3 and K_2O is much lower (1.11 and 0.52 wt.%, respectively) than that exhibited by the other three samples. This is a clear indication of the higher purity degree of SAT sand resulting from the weathering of feldspars due to a major fault affecting the Jebel Attaf series. All samples show low amounts of Fe_2O_3 (0.35–0.71 wt.%) and TiO_2 (0.29–0.72 wt.%), which are usually considered undesirable elements in glasses since they induce colouring effects. Other chromophore species like chromium are present in trace amounts and they should not influence the final colour of the glass.

The grain size cumulative curves of Barremian sands (Fig. 3) reveal unimodal distribution and prevalence of finer particles. The samples SMS, SBSA and SBJO present practically the same granulometry with a mean size approximating 150 μm when SAT sand has a courser grain size. The particle size distribution revealed a fine fraction (<2 μm) inferior to 0.4 wt.% for SMS, SBSA, SBJO and SAT, in accordance with the amount of phyllosilicates detected by semi-quantitative XRD analysis.

3.2. Geotechnical characterization and glass tests

Sands were properly mixed with the other reagents (sodium carbonate and dolomite) in order to produce glasses of fixed composition (Table 2) (wt.%): 71.91% SiO_2, 1.61% Al_2O_3, 12.52% Na_2O, 1.84% K_2O, 2.37% MgO and 9.75% CaO. Chemical analysis, carried out after firing (Table 2), shows that the oxide composition of SAT glass is very close to the theoretical expectations, while small deviations are observed in the other glasses. This is explained by the higher purity of the SAT sample, in comparison to SMS, SBSA and SBJO sands. The produced glasses can be seen in Fig. 4, while the XRD analysis (Fig. 5) confirms their completed amorphous character.

Table 2
Formulations and chemical compositions of glass materials.

	SMS glass	SAT glass	SBSA glass	SBJO glass
Sand	68.3	65.2	68.0	67.1
$CaCO_3$	5.8	6.4	5.9	6.9
Na_2CO_3	17.2	18.9	17.3	18.5
$(Mg,Ca)CO_3$	8.7	9.6	8.8	7.5
SiO_2	62.10	70.20	64.30	64.90
Al_2O_3	5.42	1.12	5.53	4.59
Fe_2O_3	0.62	0.21	0.64	0.40
MgO	1.89	1.57	1.84	1.37
CaO	11.70	12.10	10.60	11.40
Na_2O	12.70	13.40	12.10	13.20
K_2O	4.35	0.92	3.77	3.36
CuO	0.00	0.01	0.00	0.01
ZnO	0.00	0.00	0.00	0.00
Cr_2O_3	0.03	0.02	0.01	0.05
ZrO_2	0.15	0.18	0.01	0.16
TiO_2	0.52	0.30	0.58	0.21
P_2O_5	0.06	0.00	0.05	0.05
LOI	0.48	0.12	1.21	0.66
Total	100.02	100.15	100.64	100.36

Fig. 4. Soda-lime-silicate glasses produced with distinct sands.

The glass based on the SAT sand is less coloured, certainly due to the low amount of iron oxide in this sand. However, green, blue, and amber hues are also common in glass bottles or vessels, so the use of the other sands, without the need of further purification processes, is also possible.

Glasses were also characterized by scanning electron microscopy. In general, their surface is smooth and a typical

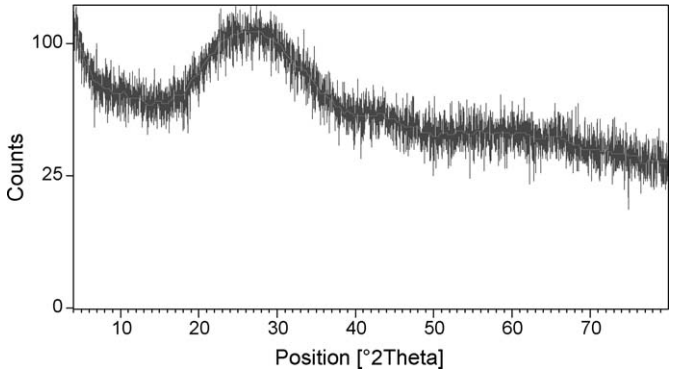

Fig. 5. XRD pattern of the glass prepared with the SMS sand.

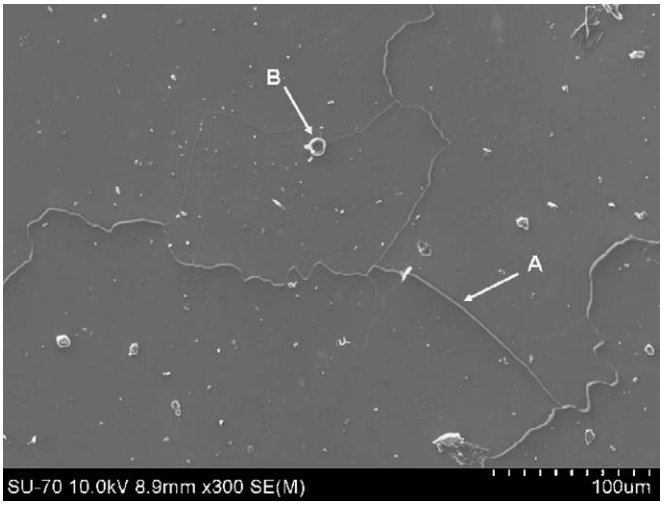

Fig. 6. Microstructure of the glass prepared with the SMS sand. (A) Microcracks and (B) gas bubbles.

homogeneous microstructure is seen, without signs of unsolved crystalline particles (see Fig. 6) [18]. Nevertheless, microcracks (signed as A in Fig. 6) are detected, probably resulting from thermal-shock tensions generated upon cooling and annealing of the glasses, as suggested by the shape of the fissures. These stages are critical in glass making and are difficult to simulate in the laboratory conditions. Moreover, some few gas bubbles (B in Fig. 6) are also observed in some glasses, denoting the need of further improvement in the firing cycle and/or the adding of refining agents to the batches.

UV–vis–IR absorption spectra of the prepared glasses are shown in Fig. 7. Two major bands in visible and NIR regions are detected and can be attributed to iron [17]. The coexistence of the two redox states of iron ions is denoted by the picks at 345 and 435 nm (associated to Fe^{3+}), while the larger band located above 600 nm and centred at 1100 nm is due to Fe^{2+} [19–21].

As referred above, iron is the major colouring impurity detected in the studied sands, affecting the optical properties of the glasses. Since iron ions might assume two redox states, Fe^{2+} and Fe^{3+}, melting conditions (namely, temperature and oxygen partial pressure of the atmosphere and batch) should be carefully controlled in order to define the following equilibrium [22]:

$$4Fe^{3+} + 2O^{2-} \leftrightarrow 4Fe^{2+} + O_2$$

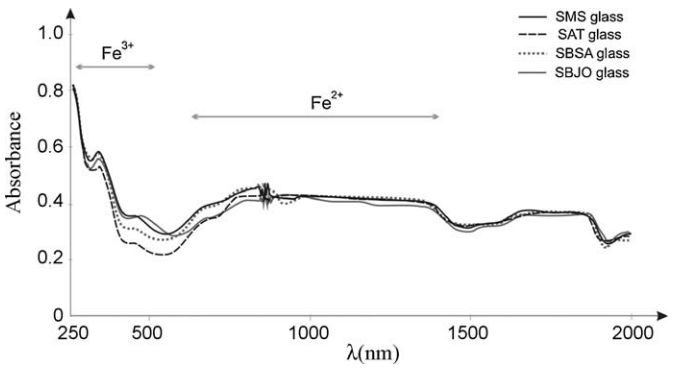

Fig. 7. UV–vis–IR spectra of the produced glasses.

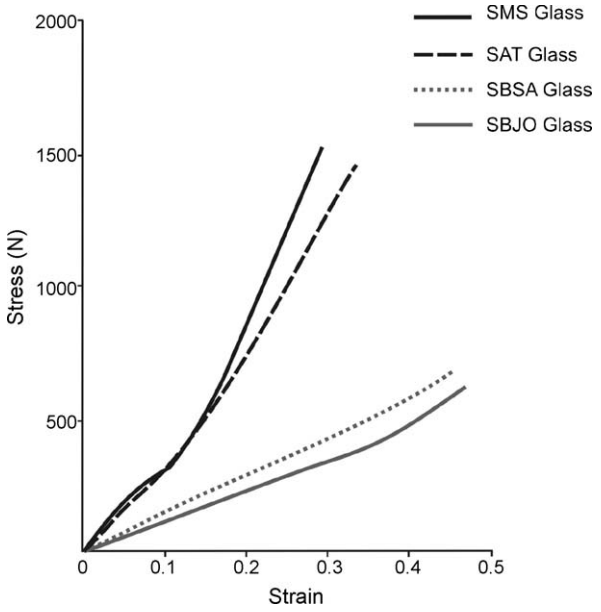

Fig. 8. Flexural stress–strain curves of glasses measured under a load of 10 kN.

The Fe^{2+}/Fe^{3+} ratio controls the glass colour changing it from green (on SMS, SAT, and SBSA based samples) to amber on SBJO based glass, where Fe^{2+} relative concentration decreases. The higher transparency of SAT glass is clearly denoted by the weakest absorbance peaks in visible region of spectra in Fig. 7. For the four glass samples, the contribution of the total amount of Fe_2O_3 to the direct evaluation of the colour intensity is minor. This oxide is mainly responsible for the glass colouration. Its dissolution in the glass matrix gives free iron species that will assume both octahedral and tetrahedral coordination. Depending on this factor and on the ferrous (Fe^{2+})/ferric iron (Fe^{3+}) ratio, the colour might change [20].

Fig. 8 shows the stress–strain curves obtained for the SMS and SBJO based glasses. The compositions based on SMS and SAT sands exhibits reasonably high flexural strength values (59.3 and 43.8 MPa, respectively). Typically, a common glass has a flexural strength of about 50 MPa [14,15]. The other two SBSA and SBJO based glasses show lower flexural strength (about 15 MPa, see also Fig. 8) due to the existence of visible cracks, that act as cleavage plans for broken. This distinct behaviour cannot be explained from differences on thermal expansion coefficients (α on insert of Fig. 9), since they are very close and also similar to values of common soda-lime glasses ($\alpha = 9.3\ 10^{-6}\ ^{\circ}C^{-1}$). Dilatometric curves reveal that softening point (560–600 °C) is observed in a region where transition from quartz α to β occurs, suggesting correct annealing procedure. These promising preliminary results confirm the potential of the materials to produce glass, but the identified defects require further studies and finer control in cooling and annealing steps.

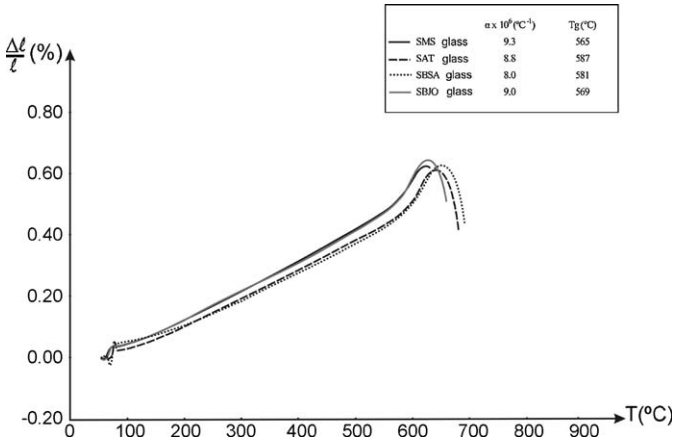

Fig. 9. Dilatometric behaviour of studied glasses.

4. Conclusions

The Barremian sands selected from central Tunisia, composed mostly of silica and feldspars, show different behaviours when tested to produce soda-lime-silica glasses. The colours exhibited by the four glass samples change from green to amber. This was due to the iron and his redox states (ferrous/ferric), as main colouring agents present in the sands. Their mechanical strength might reach suitable values, above 50 MPa. Nevertheless, only the SAT sand shows optimal aptitude to produce soda-lime glasses, due to its lower amount of iron and higher silica content. The others samples are relatively close in technological properties but they may affect the working range of automatic and semi-automatic industrial production.

References

[1] E. Le Bourhis, Glass: Mechanics and Technology, Wiley–VCH, 2007.
[2] R.H. Doremus, Glass Science, John Wiley & Sons, New York, 1973 .
[3] P.F. Burollet, Contribution à l'étude stratigraphique de la Tunisie centrale, Annales des Mines et de la Géologie 18 (1956) 352 pp.
[4] P.F. Burollet, L. Memmi, A. M'Rabet, Le Crétacé inférieur de Tunisie. Aperçu stratigraphique et sédimentologiques, Zitteliana 10 (1983) 255–264.
[5] A. M'Rabet, Stratigraphie, sédimentation et diagenèse des séries du Crétacé inférieur de Tunisie Centrale, D.Sc. Thesis, Université de Paris Sud Orsay-France, 1981, 540 pp.
[6] A. Ben Ferjani, P.F. Burollet, F. Mejri, Petroleum geology of Tunisia ETAP, Memoires Speciales (1990) 194 pp.
[7] F. Jamoussi, Etude géologique et géotechnique des substances minérales utiles de la région de Gafsa (Sud de la Tunisie), minéralogie, géochimie et application industrielle, Thèse de doctorat de spécialité en géologie, Faculté des sciences de Tunis, 1991, 298 pp.
[8] S. Bouaziz, E. Barrier, M. Soussi, M.M. Turki, H. Zouari, Tectonic evolution of the northern African margin in Tunisia from paleostress data and sedimentary record, Tectonophysics 357 (2002) 227–253.
[9] T. Zouaghi, M. Bédir, H. Abdallah, M.H. Inoubli, Seismic sequence stratigraphy, basin structuring and hydrocarbon implications of Cretaceous deposits (Albian-Maastrichtian) in central Tunisia, Cretaceous Research 30 (2009) 1–21.
[10] M. Bedir, N. Boukadi, S. Tlig, F. Ben Timzal, L. Zitouni, R. Alouani, F. Slimane, C. Bobier, F. Zargouni, Subsurface mesozoic basins in the Central Atlas of Tunisia, tectonics, sequence deposit distribution and hydrocarbon potential, American Association of Petroleum Geologists 85 (2001) 885–907.
[11] H.P. Klug, L.E. Alexander, X-ray Diffraction Procedures for Polycrystalline and Amorphous Materials, Wiley and Sons, 1974.

[12] International Centre of Diffraction Data, Powder Diffraction Data File, Version 2.16.I.C.C.D., International Centre of Diffraction Data, Newton Square, Pennsylvania, 1995.
[13] L.S. Zevin, G. Kimmel, Quantitative X-ray Diffractometry, Springer, New York, 1995, pp. 10–18.
[14] M.H. Fernandes, Introdução à Ciência e tecnologia do vidro, Universidade Aberta, 1999.
[15] F.V. Tooley, The Handbook of Glass Manufacture, vols. 1–2, Books for the Glass Industry Div., Ashlee Publishing Co., New York, 1984.
[16] M.A. Mange, H.F.W. Maurer, Heavy Mineral in Colour, Chapman & Hall, London, 1992.
[17] M.A. Mange, D.T. Wright, Heavy Minerals in Use, Developments in Sedimentology Series, vol. 58, Elsevier, 2007.
[18] S.C. Colak, E. Aral, SEM, EDX and UV spectrums of Fe_2O_3 doped soda-lime-silica glasses, Romanian Journal of Physics 50 (9–10) (2005) 1041–1046.
[19] C.R. Bamfort, Colour Generation and Control in Glass, Elsevier Scientific, Publishing Company, New York, 1977.
[20] T. Uchino, K. Nakaguchi, Y. Nagashima, T. Kondo, Prediction of optical properties of commercial soda-lime-silicate glasses containing iron, Journal of Non-Crystalline Solids 261 (2000) 72–78.
[21] C.R. Banford, Colour Generation and Control in Glass, Elsevier, Amsterdam, Netherlands, 1977.
[22] M. Yamashita, T. Akai, R. Sawa, J. Abe, M. Matsumura, Effect of preparation procedure on redox states of iron in soda-lime silicate glass, Journal of Non-Crystalline Solids 354 (2008) 4534–4538.